Indian Journal of Experimental Biology
Vol. 62, July 2024, pp. 530-539
DOI: 10.56042/ijeb.v62i07.12074

Green synthesis of calcium carbonate nano scale particles using *Benincasa hispida* (Thunb.) Cogn. pulp and their qualities

Treesa Sani[1], Sruthi VP[1], Jomol NJ[1], Nibu Varghese[2] & Soumya RS[1]*

[1]Pushpagiri Research Centre, Department of Biochemistry, Pushpagiri Institute of Medical Sciences and Research Centre, Thiruvalla, Kerala, India

[2]School of Bioscience, Mar Athanasios College For Advanced Studies (MACFAST), Thiruvalla, Kerala, India

Received 31 January 2024; *revised: 17 March 2024*

Green synthesized calcium carbonate nanoscale particles ($CaCO_3$ NPs), mainly from plant sources, have attracted much interest due to their intrinsic properties like eco-friendliness, rapidity, and cost-effectiveness. In this study, we used *Benincasa hispida* (Thunb.) Cogn. pulp was used for $CaCO_3$ NPs synthesis, and these were characterized using particle size analysis, FTIR (Fourier Transform Infrared), XRD (X-Ray Diffraction), FE-SEM (Field Emission Scanning Electron Microscopy) and EDX (Energy Dispersive X-ray). The synthesized $CaCO_3$ NPs showed good antioxidant, anti-inflammatory, and photocatalytic activity towards azodyes, i.e., TB (trypan blue) and CR (congo red). The particle size analysis showed that the $CaCO_3$ NPs have sizes from 40nm to 100µm. The FE-SEM analysis showed that the particles exist as rice-like crystals. EDX data quantified the elemental compositions of $CaCO_3$ NPs. The FTIR spectrum showed that similar functional groups of $CaCO_3$ (calcium carbonate) were present in $CaCO_3$ NPs, and XRD confirmed that these are crystalline. The in vitro antioxidant and anti-inflammatory assays were done to identify the corresponding potential of $CaCO_3$ NPs. It also displayed dye degradation potential to TB and CR. Thus, the study demonstrated that the green synthesized $CaCO_3$ NPs can be used as a potent antioxidant, anti-inflammatory, and photocatalytic agent.

Keywords: Antioxidant, Anti-inflammatory, Ash Gourd, Azodyes, Winter Melon, Wax Gourd

Nanotechnology involves processing particles to produce materials in the nano range with advanced features and uses to practice it as a tool in various fields. There is an overall increase in the implementation of nanotechnology in the medicinal field, especially in therapeutic applications. It is due to nanoparticles' high surface area and size-related properties, which can be exploited in drug delivery methods[1]. Nanoparticles have also emerged as a powerful tool in applications like targeted drug delivery, implants, diagnostic kits, and bioimaging[2]. They are used in the biomedical field due to their increased solubility, improved bioavailability, capability to cross the BBB (blood-brain barrier), pass into the pulmonary system, and absorption over the tight junctions of endothelial cells of the skin[3].

Green synthesis is an extensively used method, apart from other techniques used to prepare nanoparticles. Green synthesis is an ecofriendly method that uses biological agents, mainly plants. The phytochemicals present in the plants reduce the particles to nano-sized particles[4]. It is a cost-effective, time-saving, and cheapest method in nanoparticle synthesis. We chose the common ash gourd (*Benincasa hispida* (Thunb.) Cogn.) as the biological agent for preparation of $CaCO_3$ NPs It is an under exploited but important vegetable crop belonging to the Cucurbitaceae family[5]. Reports state its therapeutic value and use in treating many diseases like ulcers, epilepsy[6], diabetes mellitus[7], etc. Limited literature is available regarding the synthesis of $CaCO_3$ by the green method. $CaCO_3$, one of the most common biominerals, exhibits different morphologies

*Correspondence:
E-Mail: soumyapadmakumar@gmail.com

Abbreviations: BBB, Blood brain barrier; BSA, Bovine serum albumin; $CaCO_3$, Calcium carbonate; $CaCO_3$ NPs, Calcium carbonate nano scale particles; CR, Congo Red; DPPH , 2,2-Diphenyl-1-picrylhydrazyl; EA, Egg albumin; EDTA, Ethylene diamine tetra acetic acid; EDX, Energy Dispersive X-ray; $FeCl_3$, Ferric chloride; FE-SEM, Field emission scanning electron Microscopy; FTIR, Fourier transform infrared; HCl, Hydrochloric acid; H_2O_2, Hydrogen Peroxide; NADH, Nicotinamide adenine Dinucleotide hydrogen; NBT, Nitro blue tetrazolium chloride; PMS, Phenazine Methosulphate; PSA, Particle size analysis; RSA, Radical scavenging activity; SEM, Scanning electron microscopy; TB, Trypan Blue; TBA, Thiobarbituric acid; TCA, Trichloro acetic acid; SNP, Sodium nitroprusside; UV, Ultra violet; Wt%, Weight percentage; XRD, X-Ray diffraction;

in biological systems with varied functions. Because of this application, they are widely used in drug delivery and also as a diagnostic agent in disease conditions. Out of numerous nanoparticles, $CaCO_3$ NPs are constitutively used in many studies related to the biomedical field due to their availability, safety, biocompatibility, pH sensitivity, and slow biodegradability[8]. $CaCO_3$ NPs are employed in regulated drug delivery and for the encapsulation of numerous pharmaceuticals due to their ease of accessibility. $CaCO_3$ is additionally utilized as a medicine carrier and bone substitute for conditions or deformities involving the bone[9].

Possibly, it is the first report of synthesis of $CaCO_3$ NPs using *Benincasa hispida* pulp extract, its characterization using particle size analysis, XRD, FTIR, and SEM EDX, and evaluation of its antioxidant, anti-inflammatory, and dye degradation properties

Materials and Methods

All the reagents used were of analytical grade.

Sample collection and extraction

The *Benincasa hispida* pulp was collected from a nearby market in Thiruvalla, Pathanamthitta, district of Kerala. About 10 g pulp of *Benincasa hispida* was weighed, mixed with 100 mL distilled water, and incubated for 1 h at 50°C. After the incubation, the mixture was filtered using Whatman No. 1 filter paper. The filtrate was used as a plant extract. It was then stored at 4°C for further experiments.

Phytochemical screening of pulp extract

The phytochemical screening of *Benincasa hispida* pulp extract was done as per standard methods for testing the presence of alkaloids, glycosides, carbohydrate, proteins[10], flavonoids, phenolics[11], steroids[12], terpenoids, saponins[13,14] and quinones[14].

Preparation of calcium carbonate nano scale particles

$CaCO_3$ (5 g) was mixed with 50 mL of plant extract and 50 mL of distilled water (1:1 ratio) and then stirred for 30 min followed by centrifugation at 5000 rpm for 30 min. This step was repeated twice with distilled water. The pellet was then dried by keeping it in hot air oven. It was further annealed at 500°C in an electrically programmable furnace (Thermosystems India Pvt.Ltd. Thiruvananthapuram, Kerala.).

Characterization

The synthesized nano-scale particles were characterized using various methods to recognize the size, crystallinity, and shape. Firstly, the size of nano-scale particles was examined using CILAS-1180 LD (Laser diffraction particle size analyzer facility). XRD was done using Rikagu mini flex spectrometer with Kα type X-Ray generated by 600WX Ray generator to analyze the crystalline behavior of nano-scale particles. FTIR was done using an IR Prestige 21 Shimadzu spectrometer with ATR crystal zinc selenide and a resolution value of 4 cm-1 to identify the functional groups present in CaCO3 NPs. SEM EDX was done to know the morphology and elemental composition of $CaCO_3$ NPs using JSM 6390 with an accelerating voltage of 0.5 to 30 kV and magnification 300000X using tungsten filament.

Antioxidant assays

DPPH (2,2-Diphenyl-1-picrylhydrazyl) assay

The DPPH scavenging ability of $CaCO_3$ NPs was measured according to the protocol with some modifications. 50, 100, 200, 300, and 500 µg/mL sample concentrations were diluted to 1ml using methanol for the assay. About 1.4 mL DPPH was added to all the concentrations and kept in a dark room for 30 min. The absorbance was measured at 490 nm[15]. Gallic acid was used as the reference standard. The results were expressed as % radical scavenging activity (RSA) and were calculated as

$$\% \text{ of RSA} = [(A_{control} - A_{sample})/A_{control}] \times 100$$

where A_{sample} – absorbance of sample, $A_{control}$– absorbance of control.

Hydroxyl radical scavenging assay

The hydroxyl radical scavenging property of $CaCO_3$ NPs was assayed by taking different concentrations of samples ranging from 20, 50, 100, 200, 300, 400 and 500 µg/mL with minor modifications in the protocol[16]. The reaction mixture containing different concentrations of sample that is made up to 1 mL with distilled water, 800 µL phosphate buffer (50 mM, pH 7.4), 200 µL EDTA (ethylene diamine tetra acetic acid) (1.04 mM), 200 µL $FeCl_3$ (ferric chloride) (1mM), 200 µL deoxyribose (28 mM) was incubated at 37ºC for 10 minutes. After 10 min, 200 µL ascorbic acid and 200 µL H_2O_2 (hydrogen peroxide) were added and incubated at 37°C for 1 h. To this, 1.5 mL of both TBA (thiobarbituric acid) and 25% HCl (hydrochloric acid) were added. It was then kept at 100°C for 15 min and cooled. The absorbance was measured at 540 nm. The scavenging % was measured as

$$\% \text{ inhibition} = [(A_{control} - A_{sample})/A_{control}] \times 100$$

The result was calculated and expressed as IC_{50}. Catechin was taken as the standard.

Reducing power test

Reducing potential of $CaCO_3$ NPs was analyzed in accordance with the protocol with slight modifications[17]. This procedure involves combining aliquots of the sample in different concentrations (25, 50 and 100 µg/mL) with 1ml of phosphate buffer (pH 6.6) and 1mL of potassium ferricyanide (1%) in 1 mL of deionized water. For 20 minutes, the mixture was heated to 50°C in a water bath. One mL of 10% TCA (trichloroacetic acid) was added in aliquots after chilling. 0.5 mL of freshly prepared (0.1%) ferric chloride solution was added to 1 mL of the reaction mixture along with 1 mL of distilled water. The absorbance was determined using a colorimeter at 650 nm. Gallic acid was taken as the standard.

Metal chelating activity

The metal chelating potential of nano scale particles was measured by taking different concentrations of the sample (50, 100, 200, 250 and 300 µg/mL) and by adding 500 µL 2 mM ferrous chloride and 1 mL of 5 mM ferrozine to it. It was mixed well and allowed to stand at room temperature for 10 min. The absorbance was measured at 540 nm. The inhibition percentage was calculated as given below[18].

$$\% \text{ inhibition} = [(A_{control} - A_{sample})/A_{control}] \times 100$$

The result was calculated and expressed as IC_{50}. EDTA was taken as the standard.

Superoxide scavenging assay

The superoxide anion scavenging property of $CaCO_3$ NPs was measured according to the protocol with some changes[15]. The reaction mixture contained 1 mL of NBT (nitro blue tetrazolium chloride) (300 µM), 1 mL NADH (nicotinamide adenine dinucleotide hydrogen) (936 µM), 100 µL PMS (phenazine methosulphate) and 1.9 mL of different concentrations of sample (50, 100, 200 and 500 µg/mL). It was incubated at RT for 5 min. The absorbance was measured at 540 nm.

$$\% \text{ inhibition} = [(A_{control} - A_{sample})/A_{control}] \times 100$$

The superoxide scavenging property measured was estimated as IC_{50}. L-Ascorbic acid was taken as the standard.

Anti-inflammatory assays

Anti-inflammatory assay using BSA (Bovine Serum Albumin) and EA (Egg Albumin)

The anti-inflammatory potential of $CaCO_3$ NPs was checked using BSA[19,7]. The different concentrations of $CaCO_3$ NPs sample were 50, 100, 250 and 500 µg/mL. The absorbance was measured at 650 nm. The inhibition percentage was calculated as

$$\% \text{ of inhibition} = [(A_{sample}/A_{control})\text{-}1] \times 100$$

The EA assay was also done according to the method of Dharmadeva *et al*.[20]. The concentration ranging from 50, 100, 250 and 500 µg/ml of $CaCO_3$ NPs were taken. The absorbance was measured at 650 nm. The inhibition of denaturation was measured by

$$\% \text{ inhibition} = [(A_{control} - A_{sample})/A_{control}] \times 100$$

Nitric oxide assay

Nitric oxide assay was done to identify whether the nano scale particles can scavenge nitric oxide and was done according to the protocol with modifications[15]. The samples were taken in different concentrations from 50, 100, 250 and 500 µg/mL and was made up to 1 mL using distilled water. 3ml of 10 mM sodium nitroprusside (SNP) solution in phosphate buffer saline (pH 7.4) was added to all the tubes and incubated at RT for 150 min. After the incubation 0.5 mL of Griess reagent was added to all tubes, and the absorbance was measured at 540 nm. The result was calculated and expressed as IC_{50}. Quercetin was taken as the standard.

$$\% \text{ inhibition} = [(A_{control} - A_{sample})/A_{control}] \times 100$$

Photodegradation activity of $CaCO_3$ NPs on TB and CR Dye

Photodegradation assay using CR

The dye degradation potential of $CaCO_3$ NPs towards CR was done according to the protocol with modifications[21]. One mg CR was mixed with 100 mL of distilled water to make the CR dye solution. To 5 mL of the above made-up solution, 0.05 g $CaCO_3$ NPs were added and kept at RT. Another 0.05 g $CaCO_3$ NPs were added to a fresh 5 mL CR solution and irradiated with UV (ultra violet). A plain CR solution was taken as control in both cases. Absorbance was measured at an interval of 1 h and continued up to 30 h. The absorbance was measured at 590 nm. The degradation efficiency was estimated using the formula given below:

$$\% \text{ of degradation} = [(A_{control} - A_{sample})/A_{control}] \times 100$$

Photodegradation assay using TB

The procedure of TB degradation was same as that of CR degradation. 200 µL 0.4% TB dye was made up to 50 mL using distilled water. To 5 mL of the above made-up solution, 0.05 g $CaCO_3$ NPs were added and kept at RT. Another set of same samples was, kept at UV. A plain TB solution was taken as control. The absorbance was measured at an interval of 1 h and continued up to 30 h. The degradation efficiency was calculated using the formula given below:

% of degradation = $[(A_{control} - A_{sample})/A_{control}] \times 100$

Results and Discussion

Phytochemical analysis of *Benincasa hispida* pulp extract

Benincasa hispida has many health benefits because of its vitamin content, nutritional value, and minerals. As a result of its versatility, it has a vital role as an ingredient in many important food, and pharmaceutical products. Despite its advantages, no studies reported the usage of ash gourd for nano scale particle synthesis. The qualitative phytochemical examination of *Benincasa hispida* pulp extract revealed the presence of saponins, flavonoids, carbohydrates, glycosides, terpenoids, quinones, phenolics, and steroids. The presence of proteins and alkaloids was not identified in the plant extract (Table 1). It was done in-order to verify the class of compounds present in the extract that are beneficial for nano scale particles reduction. The flavonoids, and phenolics in the ash gourd extract confirmed the reducing capacity of the pulp which was important in the synthesis of nano scale particles.

Green synthesis and characterization

The mixture of $CaCO_3$ and *Benincasa hispida* pulp extracts appeared as a milky solution. A fine white powder was obtained after centrifugation and calcination of the solution. It was characterized by particle size analysis, XRD, FTIR, and SEM, EDX in order to identify the properties associated with it.

Particle size analysis

Size of nano scale particles is an essential factor for an efficient nano-carrier, as it influences the stability, cellular internalization, and other factors for the drug-loaded nanocarriers[22]. The particle size of the green synthesized $CaCO_3$ NPs (Fig. 1.) confirmed the presence of fine nano scale particles in a size range of 40 nm to 100 µm. This wide size range can be attributed to the agglomeration of $CaCO_3$ NPs in a medium. From the figure, about 80% of particles exhibit a size range of about 30-50 µm.

Table 1 — Phytochemical screening of *Benincasa hispida* pulp extract

Constituents	Test	Presence/Absence
Carbohydrates	Molisch's Test	+
Saponins	Foam Test	+
	Froth Test	+
Proteins	Ninhydrin Test	-
Alkaloids	Mayer's Test	-
	Hager's Test	-
Flavonoids	Lead Acetate Test	+
Glycosides	Keller Killiani Test	+
Terpenoids	Salkowski Test	+
Steroids	Salkowski Test	+
Phenolics	Ferric Chloride test	+
Quinone	Sulphuric Acid Test	+

XRD Analysis

The nature of $CaCO_3$ and $CaCO_3$ NPs was found to be crystalline by XRD. XRD pattern is given in Fig. 2. with significant peaks at 23°, 29°, 36°, 40°, 44°, 48° and 49°. The obtained XRD pattern was compared with green synthesized $CaCO_3$ NPs in a study by Garg *et al.*[9]. A similar XRD pattern with almost the same peaks was observed. Derkani *et al.*[23] reported that a peak at a diffraction angle 29.48° matches to a known reflection for calcite. A peak at the above-mentioned angle was observed in the greenly produced $CaCO_3$ NPs. The miller indices of the XRD pattern of $CaCO_3$ and green synthesized $CaCO_3$ NPs are bracketed against corresponding angles. These indices were compared with calcite in a study by Luo, Xianping *et al.*[24], according to their

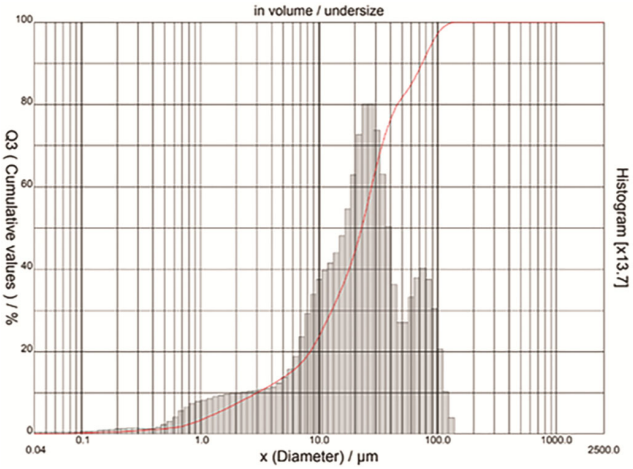

Fig. 1 — Particle size analysis of $CaCO_3$ NPs.

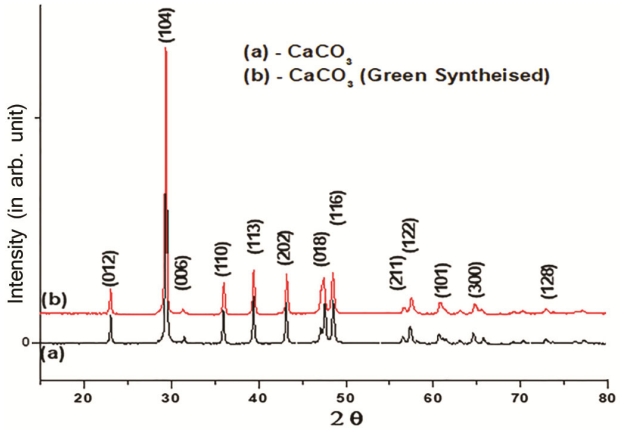

Fig. 2 — XRD data of $CaCO_3$ & $CaCO_3$ NPs with 2 theta on X axis & Intensity on Y Axis.

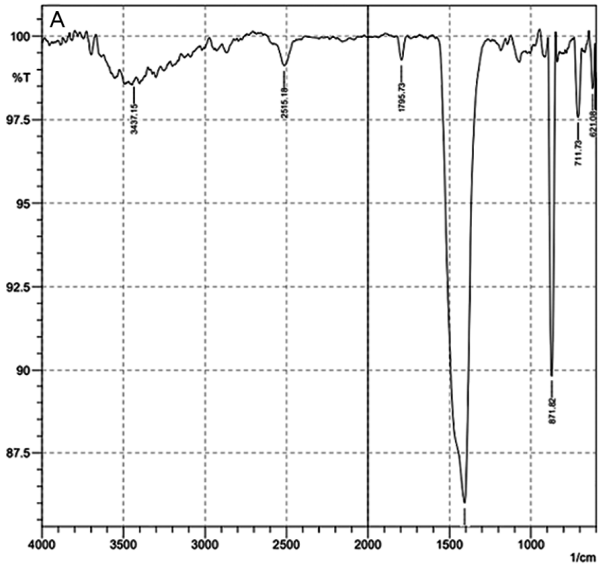

No.	Peak	Intensity	Corr. Inte	Base (H)	Base (L)	Area	Corr. Are
1	621.08	98.429	1.487	644.22	607.58	0.131	0.126
2	711.73	97.564	2.227	736.81	688.59	0.304	0.261
3	871.82	89.826	10.208	894.97	848.68	1.23	1.237
4	1408.04	86.007	13.898	1579.7	1278.81	8.914	8.798
5	1795.73	99.282	0.723	1824.66	1757.15	0.09	0.092
6	2515.18	99.12	0.68	2565.33	2457.31	0.258	0.165
7	3437.15	98.646	0.018	3439.08	3423.65	0.088	0

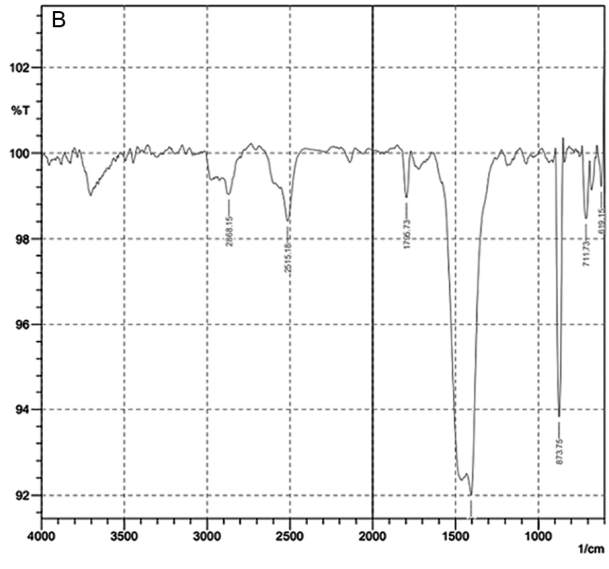

No.	Peak	Intensity	Corr. Inte	Base (H)	Base (L)	Area	Corr. Are
1	619.15	99.219	2.485	644.22	599.86	-0.013	0.277
2	711.73	98.465	1.515	734.88	690.52	0.182	0.18
3	873.75	93.823	6.402	896.9	848.68	0.717	0.765
4	1404.18	91.999	1.746	1433.11	1261.45	2.477	0.243
5	1795.73	98.959	1.131	1851.66	1768.72	0.1	0.141
6	2515.18	98.412	1.034	2553.75	2412.95	0.409	0.194
7	2868.15	99.039	0.035	2870.08	2816.07	0.134	0.005

Fig. 3 — FTIR analysis with a scan range of 600 to 4000 cm^{-1} of (a) $CaCO_3$ & (b) $CaCO_3$ NPs.

report, calcite has indices 012, 104, 006, 110, 113, 202, 018 and 116 at corresponding angles which is in agreement to the indices of the resulted XRD pattern.

FTIR analysis

Figure 3 A & B shows the FTIR spectra of $CaCO_3$, and $CaCO_3$ NPs with a scan range of 600 to 4000 cm^{-1}. The $CaCO_3$ FTIR pattern shows vibration bands at 621, 711, 871, 1408, 2980, 2875, and 2515 and 1795 cm^{-1}. Likewise, FTIR pattern of $CaCO_3$ NPs has peaks at 619, 711, 873, 1404, 1795, 2515 and 2868 cm^{-1}. When compared with a study by Charde *et al.*[25], it was confirmed that bands at 1404, 711, 871, 1408 and 873 cm^{-1} of $CaCO_3$ and $CaCO_3$ NPs FTIR spectra indicate vibration of bonds of carbonate. In a study by Garg *et al.*[9], it was reported that a sharp band at 1061, 870 and 718 cm^{-1} can be attributed to calcite polymorph, and also, a strong band at 1400 cm^{-1} corresponds to the polymorph aragonite. Green synthesized $CaCO_3$ NPs have peaks at 711, 873 and 1404 cm^{-1} that is in accord with the peaks from the above-mentioned study[9].

SEM- EDX analysis

SEM analysis (Fig. 4D.) indicates that the green synthesized $CaCO_3$ NPs consist of small-rice like crystals. A size reduction can be observed from the SEM images of nano scale particles when compared with that of original $CaCO_3$ (Fig 4B). Also, it is clear from the results that there is agglomeration between the particles. SEM image almost identical to the synthesized $CaCO_3$ NPs was obtained from a study conducted by Chaliulina *et al.*[26] (2023). As stated in their study, the SEM image corresponds to monohydrocalcite[26].

The EDX analysis permitted visualization of the elemental composition of the $CaCO_3$ and $CaCO_3$ NPs. According to the EDX data of $CaCO_3$, it contains 22.34 Wt% (weight percent) calcium, 46.4 Wt% oxygen, 30.62 Wt% carbon and 0.65 Wt% magnesium. The EDX data of $CaCO_3$ NPs showed 40.99 Wt% calcium, 48.43 Wt% oxygen, 9.98 Wt% carbon, and 0.6 Wt% magnesium. The EDX data of both compounds showed a strong signal for calcium elements. The EDX analysis of original $CaCO_3$ (Fig. 4E) also presented a strong signal for carbon, and oxygen atom. However, in the case of $CaCO_3$ NPs, there was only a weak signal for both carbon and oxygen elements. The carbon element is reduced when it comes to nano scale particles, and the calcium elements has increased when it comes to nano scale particles (Fig. 4F). Both samples contain minor traces of magnesium. No other significant difference is seen from the EDX data of original $CaCO_3$ and $CaCO_3$ NPs.

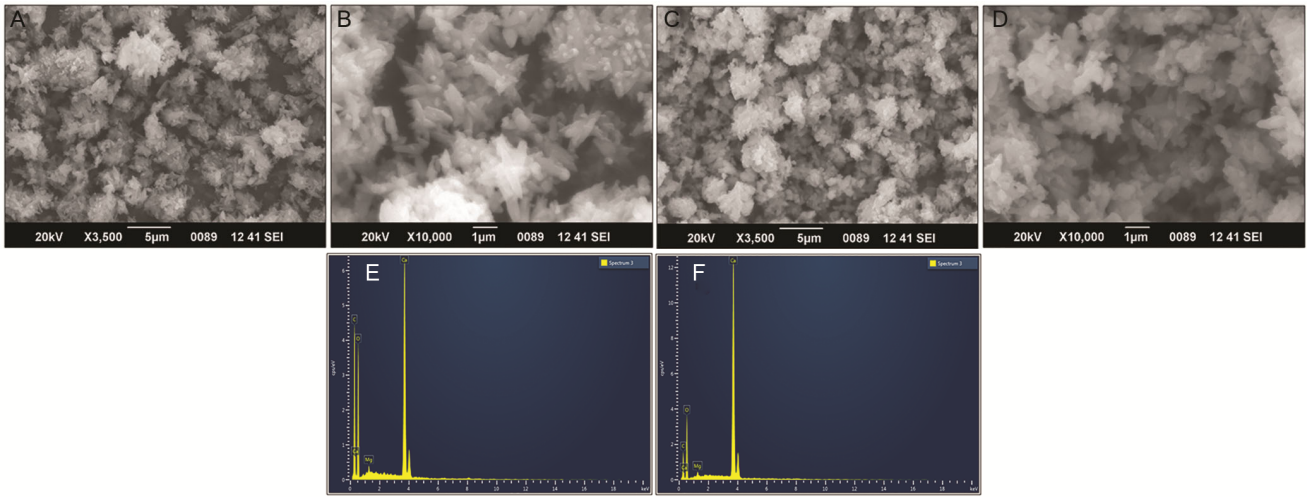

Fig. 4 — SEM Image of (A & B) $CaCO_3$ at scale bar 5 and 1 µm; and (C & D) $CaCO_3$ NPs at 5 and 1µm, respectively; and (E & F) EDX data of $CaCO_3$ and $CaCO_3$ NPs.

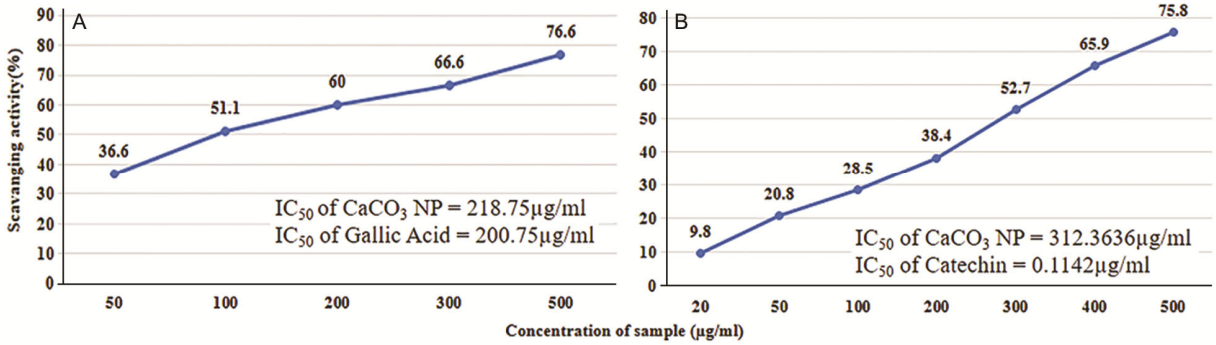

Fig. 5 — Antioxidant potential of $CaCO_3$ NPs (A) DPPH assay; and (B) Hydroxyl radical assay.

Assessment of antioxidant activities

DPPH and hydroxyl radical scavenging assay

The radical scavenging activity of the $CaCO_3$ NPs was assessed by DPPH assay. DPPH test is a standard assay to evaluate samples' radical scavenging capability. DPPH has a purple color with an absorbance at 490 nm in methanol; hence, scavenging the DPPH will result in a decline in absorbance[27,28]. From this assay, it was revealed that the $CaCO_3$ NPs (50, 100, 200, 300 and 500 µg/mL) have antioxidant properties with an IC_{50} value of 218.73 µg/mL. Gallic acid was used as the standard at varying concentrations (10, 50, 100, 200 and 300 µg/mL). The standard gallic acid has IC_{50} 200.75 µg/mL (Fig. 5A). A dose-dependent increase in the scavenging activity of DPPH was seen in $CaCO_3$ NPs.

Hydroxyl radicals are radicals that can induce harmful effects on the major macromolecules like nucleic acids in biological systems[29]. This assay was conducted to check the hydroxyl radical scavenging ability of $CaCO_3$ NPs. In this experiment, hydroxyl radicals are produced by Fenton reaction between ferrous ion and hydrogen peroxide. Different probes, like deoxyribose, and benzoate have used colorimetric measures to show the damage produced by hydroxyl radicals. The deoxyribose probe gets degraded in the presence of hydroxyl radical, and forms a pink chromogen upon heating with TBA. The probe is protected from the hydroxyl radicals by the radical scavengers present in the sample[30]. Catechin was chosen as the standard. The samples showed the scavenging activity in a concentration dependent manner as seen in the figure (Fig. 5B). For $CaCO_3$ NPs 312.363 µg/mL is the IC_{50}, and that of catechin is 0.1142 µg/mL. Compared to catechin; $CaCO_3$ NPs have moderate scavenging activity, and can be considered to have antioxidant potential.

Various inorganic nanoparticles have shown antioxidant activity toward DPPH, and hydroxyl radicals. There were no available reports stating the

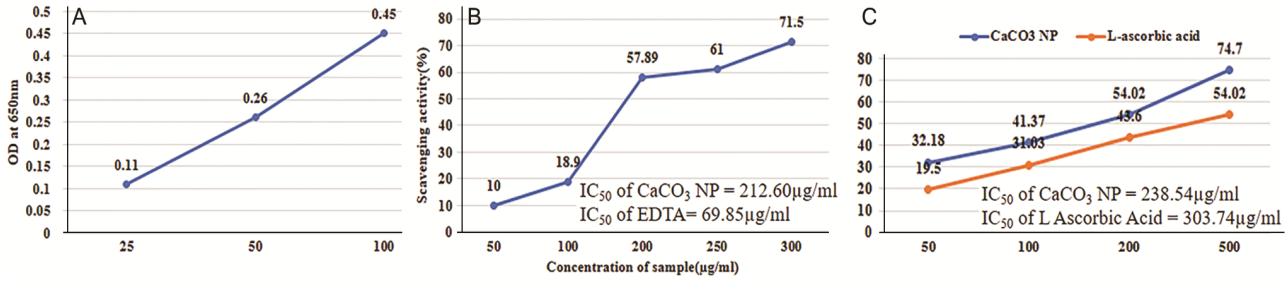

Fig. 6 — Antioxidant ability of $CaCO_3$ NPs (A) Total reducing power assay; (B) Metal chelating assay; and (C) Superoxide scavenging assay.

antioxidant potential of $CaCO_3$ NPs and only few reports stating the antioxidant potential of $CaCO_3$ are available[31]. However, antioxidant potential of nano scale particles can be enhanced by conjugating natural compounds.

Reducing power assay, metal chelation assay and superoxide radical scavenging assay

The principle behind the reducing power assay is that compounds having reducing power combine with Fe^{3+} to generate Fe^{2+}, which then reacts with ferric chloride to produce ferric-ferrous complex, which has an absorbance at 650 nm[27]. The total reducing potential of the samples and gallic acid were carried out at concentrations 20, 50 and 100 µg/mL. The gallic acid showed 0.54 absorbance at a concentration of 50 µg/mL, and the $CaCO_3$ NPs showed an absorbance of 0.26 at 50 µg/mL. As indicated in the Fig. 6A, the reduction power of $CaCO_3$ NPs is increased by a rise in concentration of nano scale particles.

Metal chelating potential of $CaCO_3$ NPs was assayed by its potential to disrupt the formation of a red ferrous ion-ferrozine complex in the reaction mixture. Ferrozine can quantitatively form complexes with Fe^{2+} ions. In the presence of other chelating agents, the complex formation would be disrupted which result in the decrease in the red colour[32]. As shown in Fig. 6B, the metal chelating test results demonstrate that $CaCO_3$ NPs have good metal chelation capacity. The standard solution EDTA, showed maximum Fe^{2+} ion chelating activity (75.17%) at higher concentrations (100 µg/mL). Also, the Fe^{2+} ion chelating power for $CaCO_3$ NPs at 100 µg/mL was observed to be 18.9% from the figure.

The superoxide radical scavenging (O^{2-}) assay involves using O^{2-} which is produced through different reaction methods. PMS is used to oxidize NADH to produce O^{2-}. The probe chosen to quantitate O^{2-} was NBT. NBT is reduced to a purple-coloured formazan by O^{2-} [33]. Figure 6C summarizes the scavenging effects of $CaCO_3$ NPs produced from *Benincasa hispida* pulp extract within a concentration range from 50, 100, 200 and 500 µg/mL. The samples had scavenged superoxide in a concentration-dependent manner. The standard taken was L-ascorbic acid. The L ascorbic acid shows superoxide scavenging activity with IC_{50} value of 303.7394 µg/mL. The IC_{50} of $CaCO_3$ NPs was found to be 238.5493 µg/mL. The Fig. 6C reveals that $CaCO_3$ NPs had the highest scavenging activity towards superoxide anion radicals at a concentration of 500 µg/mL.

Anti-inflammatory assays

Anti-inflammatory assay using BSA, EA and nitric oxide assay

Protein denaturation can be considered to be one of the causes of inflammation. As a result, agents or chemicals that significantly reduce protein denaturation may have potential anti-inflammatory effects[34]. BSA and EA were taken to check whether the test samples prevent its denaturation. Evaluation of anti-inflammatory activity was done at different concentrations of $CaCO_3$ NPs i.e., 50, 100, 250 and 500 µg/mL. However, the standard, diclofenac sodium (100, 200, 300 and 400 µg/mL) with IC_{50} of 221.01 µg/mL showed an 89% inhibition at 400 µg/mL. $CaCO_3$ NPs at concentration (500 µg/mL) exhibited the highest level of anti-inflammatory activity at 75% inhibition for BSA assay with an IC50 of 329.80 µg/mL (Fig. 7A).

Anti-inflammatory potential of $CaCO_3$ NPs was also assessed against denaturation of EA method. The highest inhibition rate of $CaCO_3$ NPs was observed at the concentration of 500 µg/mL. Our green synthesized $CaCO_3$ NPs at concentration (50, 100, 250 and 500 µg/mL) exhibited the highest level of anti-inflammatory activity at 59% inhibition for EA assay (Fig. 7B). For $CaCO_3$ NPs 422.0103 µg/mL is the IC_{50}. When compared to standard diclofenac sodium having 89% of inhibition at 400 µg/mL, the inhibiting activity of EA denaturation is very low for $CaCO_3$ NPs.

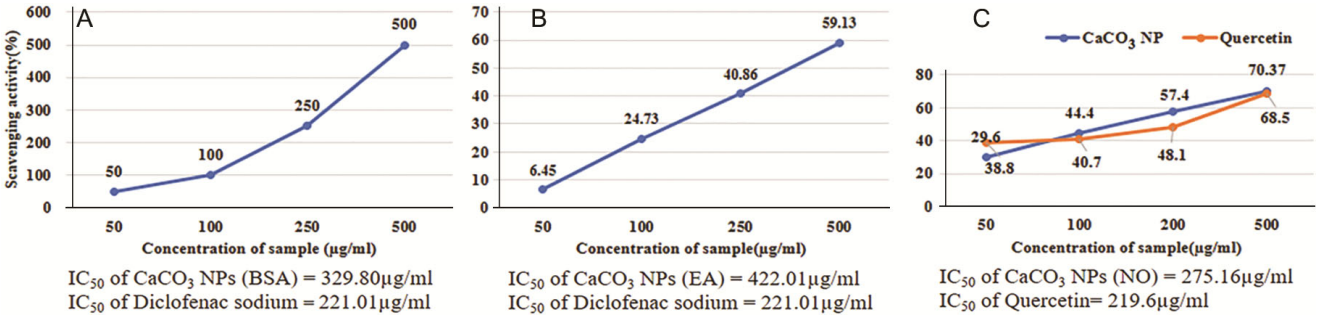

Fig. 7 — Anti-inflammatory activity of $CaCO_3$ NPs against denaturation of (A) BSA; (B) EA; and (C) Nitric oxide scavenging property of $CaCO_3$ NPs.

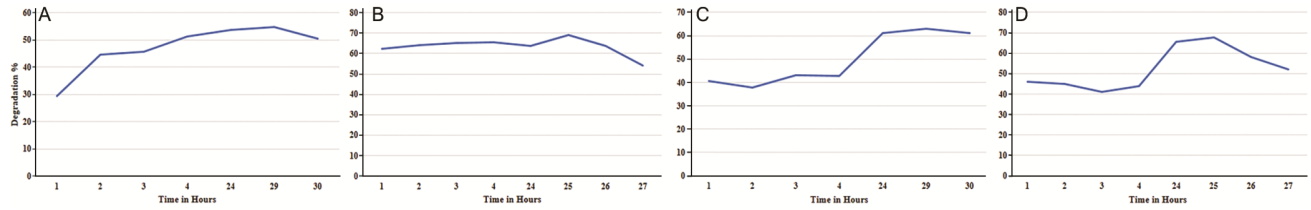

Fig. 8 — Photocatalytic effect of $CaCO_3$ NPs against 9A & B) CR at normal temperature and UV irradiation; and (C & D) TB at normal temperature and UV irradiation

Nitric oxide has an important role in the pathogenesis of inflammation. Nitric oxide is generated during inflammation as a mediator with response to the activation of immune cells. The interaction of nitric oxide with toxic agents will lead to many disease conditions. It is a signaling molecule that is involved in immune system, neurotransmission and vasodilation, etc. It has been studied that inflammation can be regulated by the suppression of nitric oxide production[35]. This test helps to measure the scavenging potential of nitric oxide by $CaCO_3$ NPs. The standard taken was quercetin in increasing concentrations of 50, 100, 200 and 500 µg/mL. The IC_{50} value of quercetin was 219.6 µg/mL. The $CaCO_3$ NPs were taken in the same concentration as that of standard. The estimated value of IC_{50} was found to be 275.16 µg/mL in $CaCO_3$ NPs (Fig. 7C). Compared to quercetin; the nano scale particles are slightly less efficient than quercetin in scavenging nitric oxide.

From these assays it was revealed that $CaCO_3$ NPs have anti-inflammatory activity, which makes it promising for future, and can be used as an anti-inflammatory agent. $CaCO_3$ NPs can be generated as an anti-inflammatory drug after necessary studies in *in vitro* cell line and in *in vivo* studies. A work by Jung *et al*.[36] had studied about the anti-inflammatory properties of tannylated $CaCO_3$ NPs. In their study they had conjugated tannic acid which have anti-inflammatory properties with $CaCO_3$ NPs, and checked the expression of pro-inflammatory factors in lipopolysaccharide stimulated chondrocytes. Clinical study reports are also available that had described the anti-inflammatory activity of $CaCO_3$ by discovering the down regulation of pro-inflammatory cytokines[37].

Photocatalysis of $CaCO_3$ NPs

Photocatalytic activity of the greenly made $CaCO_3$ NPs was studied by degradation of CR and TB under UV irradiation and at normal RT. The degradation of the dyes in presence of $CaCO_3$ NPs was confirmed by the continual decrease of its absorption peak intensity within 30 h of observation. The control showed almost no change of colour within the observation period. The nano scale particles had shown decent photocatalytic activity towards azo dyes specifically towards CR and TB under both UV and normal temperature conditions. It was observed that these dye particles were adsorbed onto the surface of these nano scale particles within hours thus obtaining almost clear solution. This property of $CaCO_3$ NPs can be used in various applications like dye removal, therapeutic and diagnostic purposes etc. The maximum percentage of degradation was 50% on CR in RT and 54% in UV (Fig. 8 A & B). In case of TB, it was 61% in room temperature and 52% in UV (Fig. 8 C & D). After 30 h of duration, this particular reaction mixture had attained equilibrium thereby not any further degradation of dye.

Although many inorganic nanoparticles have shown the dye degradation potential, only a few studies about photocatalysis have been conducted on $CaCO_3$ NPs. One such study by Ghadiri *et al*.[38] had made use of $CaCO_3$ NPs for methylene blue degradation. They had reported about 93% degradation of methylene blue by $CaCO_3$ NPs within 2 h thereby affirming the photocatalytic ability of $CaCO_3$ NPs. Another study involving the use of $CaTiO_3$ nanoparticles from $CaCO_3$ NPs and TiO_2 on the degradation of Brilliant green dye was done by Ernawati *et al*.[39]. They had evaluated the impact of concentration of dye and photocatalyst on dye degradation. It was stated in their study that the dye molecules were chemisorbed onto the surface of photocatalyst. The green synthesized $CaCO_3$ NPs has also exhibited similar results of photocatalysis which is in line with the above-mentioned studies.

Conclusion

The present work describes the green synthesis of $CaCO_3$ NPs using the *Benincasa hispida* (ash gourd) pulp extract. The pulp extract was analyzed for phytochemical compounds and had shown the presence of various secondary metabolites including phenolics and flavonoids. It had been successful in generating nano scale particles of $CaCO_3$ through various characterization techniques with antioxidant, anti-inflammatory and photocatalytic activities. Thus the future studies involve the usage of $CaCO_3$ NPs in drug delivery applications.

Acknowledgement

We would like to acknowledge Dr. Jomit T Mathew. SB College Changanacherry, for XRD studies; Dr. Padmakumar, Head, Dept. of Physics, MG College, Thiruvananthapuram, for analysis of XRD data; Mr. Akhil Nazim M K Dept. of Environmental Science, MG University, Kottayam, for FTIR studies; Dr. Reji Srinivas, Scientist, and Mr. Sreeraj M K Marine Geoscience Group, National Centre for Earth Science Studies, Thiruvananthapuram for particle size analysis; and DST-SAIF Cochin and its faculties for the SEM EDX analysis.

Conflict of Interest

Authors declare no competing interests.

References

1 Abaszadeh F, Ashoub MH, Khajouie G & Amiri M, Nanotechnology development in surgical applications: recent trends and developments. *Eur J Med Res*, 28 (2023) 1.

2 Sim S & Wong NK, Nanotechnology and its use in imaging and drug delivery (Review). *Biomed Rep*, 14 (2021) 42.

3 Chenthamara D, Subramaniam S, Ramakrishnan SG, Krishnaswamy S, Essa MM, Lin FH & Qoronfleh MW, Therapeutic efficacy of nanoparticles and routes of administration. *Biomater Res*, 23 (2019) 20.

4 Tarannum N, Divya & Gautam YK, Facile green synthesis and applications of silver nanoparticles: a state-of-the-art review. *RSC Adv*, 9 (2019) 34926.

5 Gupta P, Chikkala S & Kundu P, Ash gourd and its applications in the food, pharmacological and biomedical industries. *Int J Veg Sci*, 27 (2021) 44.

6 Islam MT, Quispe C, El-Kersh DM, Shill MC, Bhardwaj K, Bhardwaj P, Sharifi-Rad J, Martorell M, Hossain R, Al-Harrasi A, Al-Rawahi A, Butnariu M, Rotariu LS, Suleria HAR, Taheri Y, Docea AO, Calina D & Cho WC, A Literature-Based Update on Benincasa hispida (Thunb.) Cogn.: Traditional Uses, Nutraceutical, and Phytopharmacological Profiles. *Oxid Med Cell Longev*, 2021 (2021) 1.

7 Palamthodi S, Kadam D & Lele SS, Physicochemical and functional properties of ash gourd/bottle gourd beverages blended with jamun. *J Food Sci Technol*, 56 (2019) 473.

8 Zhao P, Tian Y, You J, Hu X & Liu Y, Recent Advances of Calcium Carbonate Nanoparticles for Biomedical Applications. *Bioengineering* (Basel), 9 (2022) 691.

9 Garg R, Kumari M, Kumar M, Dhiman S & Garg R, Green synthesis of calcium carbonate nanoparticles using waste fruit peel extract. *Mater Today: Proc*, 46 (2021) 6665.

10 Kancherla N, Dhakshinamoothi A, Chitra K & Komaram RB, Preliminary analysis of phytoconstituents and evaluation of anthelminthic property of Cayratia auriculata (*in vitro*). *Maedica*, 14 (2019) 350.

11 Singh PK, Singh J, Medhi T & Kumar A, Phytochemical Screening, Quantification, FT-IR Analysis, and *In Silico* Characterization of Potential Bio-active Compounds Identified in HR-LC/MS Analysis of the Polyherbal Formulation from Northeast India. *ACS Omega*, *7* (2022) 33067.

12 Chen M, He X, Sun H, Sun Y, Li L, Zhu J, Xia G, Guo X & Zang H, Phytochemical analysis, UPLC-ESI-Orbitrap-MS analysis, biological activity, and toxicity of extracts from Tripleurospermum limosum (Maxim.) Pobed. *Arab J Chem*, 15 (2022) 1.

13 Dahanayake JM, Perera PK, Galappatty P, Perera HDSM & Arawwawala LDAM, Comparative Phytochemical Analysis and Antioxidant Activities of Tamalakyadi Decoction with Its Modified Dosage Forms. *Evid Based Complement Alternat Med*, 2019 (2019) 1.

14 Magar AB, Shrestha D, Pakka S & Sharma KR, Phytochemistry, Biological, and Toxicity Study on Aqueous and Methanol Extracts of Chromolaena odorata. *ScientificWorldJournal* 2 (2023) 1.

15 Pal A, Chouni A, Das A, Ray R & Paul S, Evaluation of anti-proliferative potential and antioxidant activity of a wild edible mushroom Macrocybe crassa (Sacc.) pegler and lodge. *Pharmacogn J*, 11 (2019) 1504.

16 Fejér J, Kron I, Pellizzeri V, Pľuchtová M, Eliašová A, Campone L, Gervasi T, Bartolomeo G, Cicero N, Babejová A, Konečná M, Sedlák V, Poráčová J & Gruľová D, First Report on Evaluation of Basic Nutritional and Antioxidant Properties of Moringa Oleifera Lam. from Caribbean Island of Saint Lucia. *Plants* (Basel), 8 (2019) 537.

17 Ayoub L, Hassan F, Hamid S, Abdelhamid Z, & Souad, A, Phytochemical screening, antioxidant activity and inhibitory potential of Ficus carica and Olea europaea leaves. *Bioinformation*, 15 (2019) 226.

18 Gulcin İ & Alwasel SH, Metal Ions, Metal Chelators and Metal Chelating Assay as Antioxidant Method. *Processes*, 10 (2022) 132.

19 Banerjee S, Chanda A, Adhikari A, Das AK & Biswas S, Evaluation of phytochemical screening and anti-inflammatory activity of leaves and stem of Mikania scandens (L.) wild. *Ann Med Health Sci Res*, 4 (2014) 532.

20 Dharmadeva S, Galgamuwa LS, Prasadinie C & Kumarasinghe N, *In vitro* anti-inflammatory activity of Ficus racemosa L. bark using albumin denaturation method. *Ayu*, 39 (2018) 239.

21 Vasiljevic ZZ, Dojcinovic MP, Vujancevic JD, Jankovic-Castvan I, Ognjanovic M, Tadic NB, Stojadinovic S, Brankovic GO & Nikolic MV, Photocatalytic degradation of methylene blue under natural sunlight using iron titanate nanoparticles prepared by a modified sol–gel method. *Royal Soc Open Sci*, 7 (2020) 1.

22 Haque ST, Islam RA, Gan SH & Chowdhury EH, Characterization and evaluation of bone-derived nanoparticles as a novel pH-responsive carrier for delivery of doxorubicin into breast cancer cells. *Int J Mol Sci*, 21 (2020) 1.

23 Derkani MH, Fletcher AJ, Fedorov M, Abdallah W, Sauerer B, Anderson J & Zhang ZJ, Mechanisms of surface charge modification of carbonates in aqueous electrolyte solutions. *Colloids Interfaces*, 3 (2019) 62.

24 Luo X, Song X, Cao Y, Song L & Bu X, Investigation of calcium carbonate synthesized by steamed ammonia liquid waste without use of additives. *RSC Adv*, 10 (2020) 7976.

25 Charde SJ, Sonawane SS, Sonawane SH & Navin S, Influence of functionalized calcium carbonate nanofillers on the properties of melt-extruded polycarbonate composites. *Chem Eng Commun*, 205 (2018) 492.

26 Chaliulina R, On Sustainable Production of $CaCO_3$ via Monohydrocalcite—A Carbon Capture and Mineralisation Product from Waste Brines. *Green Sustain Chem*, 13 (2023) 34.

27 Vasyliev GS, Vorobyova VI & Linyucheva OV, Evaluation of Reducing Ability and Antioxidant Activity of Fruit Pomace Extracts by Spectrophotometric and Electrochemical Methods. *J Anal Methods Chem*, 2020 (2020) 1.

28 Baliyan S, Mukherjee R, Priyadarshini A, Vibhuti A, Gupta A, Pandey RP & Chang CM, Determination of antioxidants by DPPH radical scavenging activity and quantitative phytochemical analysis of Ficus religiosa. *Molecules*, 27 (2022) 1.

29 Ali A, Mashwani Z-U-R, Raja NI, Mohammad S, Ahmad MS & Luna-Arias JP, Antioxidant and Hypoglycemic Potential of Phytogenic Selenium Nanoparticle- and Light Regime-Mediated In Vitro Caralluma tuberculata Callus Culture Extract. *ACS Omega*, 9 (2024) 20101.

30 Sadeer BN, Montesano D, Albrizio S, Zengin G & Mahomoodally MF, The Versatility of Antioxidant Assays in Food Science and Safety-Chemistry, Applications, Strengths, and Limitations. *Antioxidants* (Basel), 9 (2020) 709.

31 Wang L, Wang X, Guo Z, Xia Y, Geng M, Liu D, Zhang Z & Yang Y, Nano-Microemulsions of $CaCO_3$-Encapsulated Curcumin Ester Derivatives With High Antioxidant and Antimicrobial Activities and pH Sensitivity. *Front Vet Sci*, 9 (2022) 1.

32 Gulcin İ & Alwasel SH, Metal Ions, Metal Chelators and Metal Chelating Assay as Antioxidant Method. *Processes*, 10 (2022) 132.

33 Apak R, Calokerinos A, Gorinstein S, Segundo M, Hibbert D, Gülçin İ, Demirci Çekiç S, Güçlü K, Özyürek M, Çelik S, Magalhães L & Arancibia-Avila P, Methods to evaluate the scavenging activity of antioxidants toward reactive oxygen and nitrogen species (IUPAC Technical Report). *Pure Appl Chem*, 94 (2022) 87.

34 Mendez-Encinas MA, Valencia D, Ortega-García J, Carvajal-Millan E, Díaz-Ríos JC, Mendez-Pfeiffer P, Soto-Bracamontes CM, Garibay-Escobar A, Alday E & Velazquez C, Anti-Inflammatory Potential of Seasonal Sonoran Propolis Extracts and Some of Their Main Constituents. *Molecules*, 28 (2023) 1.

35 Inkanuwat A, Sukaboon R, Reamtong O, Asawanonda P, Pattaratanakun A, Saisavoey T, Sangtanoo P & Karnchanatat A, Nitric oxide synthesis inhibition and anti-inflammatory effect of polypeptide isolated from chicken feather meal in lipopolysaccharide-stimulated RAW 264.7 macrophages. *Food Technol Biotechnol*, 57 (2019) 200.

36 Jung SY, Hwang H, Jo HS, Choi S, Kim HJ, Kim SE & Park K, Tannylated calcium carbonate materials with antacid, anti-inflammatory, and antioxidant effects. *Int J Mol Sci*, 22 (2021) 1.

37 Díaz-De la Cruz EN, Cerrillos-Gutiérrez JI, García-Sánchez A, Prado-Nevárez CG, Andrade-Sierra J, Jalomo-Martínez B, Banda-López A, Rojas-Campos E & Miranda-Díaz AG, The Influence of Sevelamer Hydrochloride and Calcium Carbonate on Markers of Inflammation and Oxidative Stress in Hemodialysis at Six Months of Follow-Up. *Front Med*, 8 (2021) 1.

38 Ghadiri Soltan Meydan T, Samareh Moosavi S, Sabouri Z & Darroudi M, Green synthesis of CaCO3 nanoparticles for photocatalysis and cytotoxicity. *Bioprocess Biosyst Eng*, 46 (2023) 727.

39 Ernawati L, Wahyuono RA, Widiyandari H, Risanti DD, Yusariarta AW, Rebeka & Sitompul V, Experimental data of $CaTiO_3$ photocatalyst for degradation of organic pollutants (Brilliant green dye)–Green synthesis, characterization and kinetic study. *Data Brief*, 32 (2020) 1.